

INTER-GRAIN EXCHANGE INTERACTION AND HYSTERESIS LOOPS
OF MELT-SPUN $\text{Nd}_{13}\text{Fe}_{77}\text{B}_{10}$

Jin Han-min^{*,***}, Y.B.Kim^{*}, W.S.Park^{**}, M.J.Park^{**}, and Li Tian^{***}

^{*} Korea Research Institute of Standards and Science, Taejeon 305-606, Korea

^{**} Korea University, Seoul, Korea

^{***}Department of Physics, Jilin University, Changchun, 130023, P.R.China

It is believed in general that the domain wall pinning at the grain boundaries is the origin of high coercivity of melt-spun Nd-Fe-B permanent magnet [1-2]. For near-stoichiometric alloys, J_r increases beyond $J_s/2$ and iH_c decreases with decrease of the scale of the nanostructure [3], which is ascribed to the inter-grain exchange interaction [4]. This work presents new evidences of the inter-grain exchange interaction, and shows that the magnetization process of the melt-spun $\text{Nd}_{13}\text{Fe}_{77}\text{B}_{10}$ is the non-coherent magnetization rotation of the grains.

A melt-spun alloy of $\text{Nd}_{13}\text{Fe}_{77}\text{B}_{10}$ was annealed at 950 K (specimen #1) or 970 K (specimen #2) for 10 minutes. The specimens are essentially single phase of $\text{Nd}_2\text{Fe}_{14}\text{B}$. The hysteresis loops were measured after cooled down at remanent state.

The model magnet is composed of $n \times n \times n$ cubic $\text{Nd}_2\text{Fe}_{14}\text{B}$ grains. Both of the c- and [100]-axes of the grains are randomly oriented. Each grain is exchange coupled with the six adjacent grains. Each grain consists of $m \times m \times m$ cubic elements of equal dimension L/m . The periodic boundary conditions hold for the magnet. The magnetization of the magnet was obtained from minimization of the total energy consisting of the magnetocrystalline anisotropy energy, Zeeman energy and the exchange energy $-wL^2/2\mu_0m^2 \sum_{i,j} \vec{J}_s(i) \cdot \vec{J}_s(j)$. The value of w/L was obtained fitting the computation of iH_c at 4.2 K. $m=1$ and $w=0$, $m=1$ and $w \neq 0$, and $m > 1$ and $w \neq 0$ correspond to the S-W model, the exchange coupled SD model, and micromagnetism, respectively.

Figures 4a, 5a and 6a show the experimental hysteresis loops for specimens #2 (4a) and #1 (5a and 6a). Figures $n\alpha$ ($\alpha=b,c,d$) are the simulation of the corresponding experiments by the S-W model ($\alpha=b$), exchange coupled SD model ($\alpha=c$) and micromagnetism ($\alpha=d$). The micromagnetism simulates the experiments fairly well quantitatively.

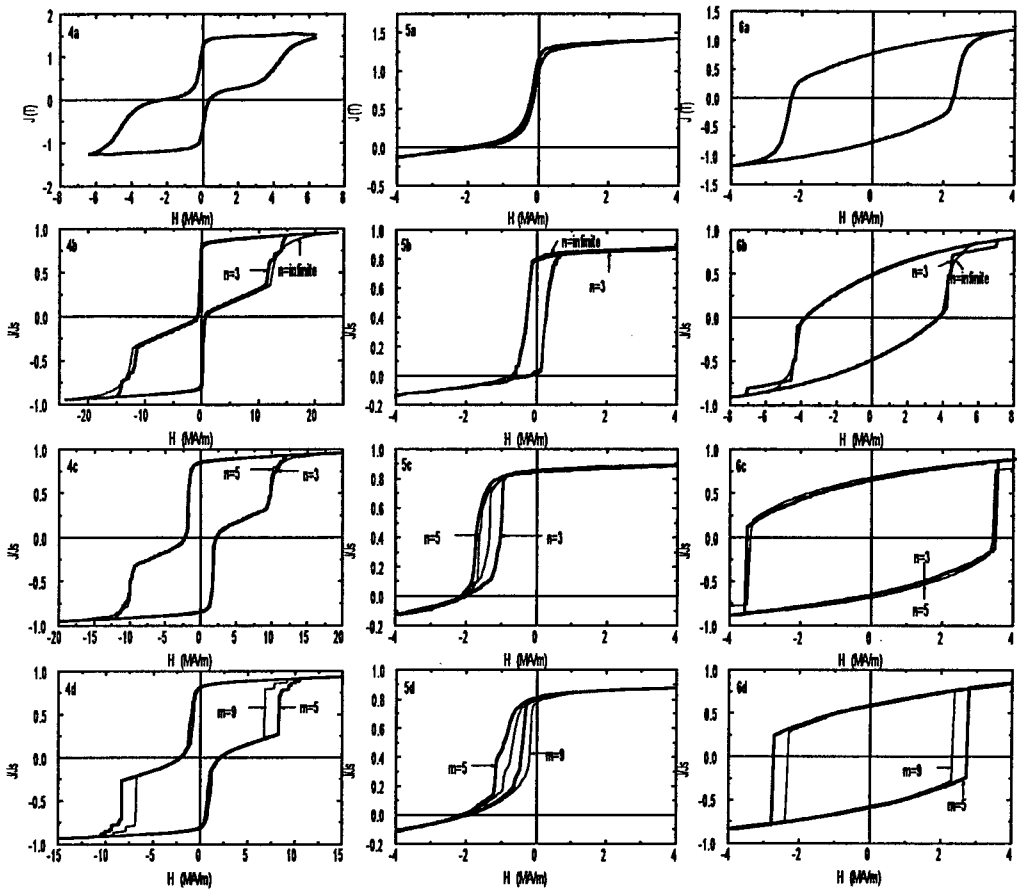


Figure 4. Hysteresis loops at 4.2 K measured in the fields of $H_{max}=6.4$ MA/m (a), and major loops computed by the S-W model for $n=3$ and ∞ (b), by the exchange coupled SD model for $n=3$ ($w/L=0.45$) and $n=5$ ($w/L=0.48$) (c), and by the micromagnetism for $n=3$ and $m=5$ ($w/L=0.32$) and $m=9$ ($w/L=0.29$) (d)

Figure 5. Hysteresis loops at 4.2 K in the fields of $H_{max}=4.0$ MA/m measured (a), and computed by the S-W model for $n=3$ and ∞ (b), by the exchange coupled SD model for $n=3$ ($w/L=0.45$) and $n=5$ ($w/L=0.48$) (c), and by the micromagnetism for $n=3$ and $m=5$ ($w/L=0.32$) and $m=9$ ($w/L=0.29$) (d)

Figure 6. Hysteresis loops at 250 K in the fields of $H_{max}=4.0$ MA/m measured (a), and major loops computed by the S-W model for $n=3$ and ∞ (b), by the exchange coupled SD model for $n=3$ ($w/L=0.45$) and $n=5$ ($w/L=0.48$) (c), and by the micromagnetism for $n=3$ and $m=5$ ($w/L=0.32$) and $m=9$ ($w/L=0.29$) (d)

REFERENCES

- [1] R. K. Mishra, J. Magn. Magn. Mater., 54-57(1986)450.
- [2] F. E. Pinkerton and C. D. Fuerst, J. Appl. Phys., 67(1990)4753.
- [3] A. Manaf, R. A. Buckley, H. A. Davies and M. Leonowicz, J. Magn. Magn. Mater., 101 (1991)360.
- [4] G. B. Clemente, J. E. Keem and J. P. Bradley, J. Appl. Phys., 64(1988)5299.